

# SYNTHESIS AND CHARACTERIZATION OF THE MICROSTRUCTURE AND FUNCTIONAL GROUP BOND OF Fe<sub>3</sub>O<sub>4</sub> NANOPARTICLES FROM NATURAL IRON SAND IN TOBELO NORTH HALMAHERA

Ferni Malega<sup>1</sup>, I Putu Tedy Indrayana\*<sup>2</sup>, Edi Suharyadi<sup>3</sup>

<sup>1</sup> Physics Study Program, Universitas Halmahera, North Maluku, Indonesia

<sup>2, 3</sup> Physics Department, Faculty of Mathematics and Science, Universitas Gadjah Mada, Yogyakarta, Indonesia

\*Correspondence address: tedyindrayana@gmail.com

Received: June 26<sup>th</sup>, 2018. Accepted: October 24<sup>th</sup>, 2018. Published: October 28<sup>th</sup>, 2018

**Abstract:** The Fe<sub>3</sub>O<sub>4</sub> nanoparticles have been successfully synthesized from natural iron sand by using coprecipitation method at a temperature of 56°C. The elemental identification, structural characterization, and bonding analysis were carried out using XRF, XRD, and FTIR, respectively. The sample nanoparticles contain elements of Al, P, Ca, Ti, V, Cr, Mn, Ni, Cu, Zn, Rb, Re, Bi, and Fe. The composition of Fe element is 87.37%. The sample of the nanoparticle exhibited as the Fe<sub>3</sub>O<sub>4</sub> which was shown by the diffraction pattern that belongs to a cubic spinel structure of Fe<sub>3</sub>O<sub>4</sub>. The crystallite size of the nanoparticle is 42.25 ± 0.42 nm. The lattice parameter was found at 8.384 ± 0.049 Å. The crystallite density is 5.232 × 10<sup>3</sup> kg/m<sup>3</sup> while the lattice strain is 1.413 × 10<sup>-3</sup>/line. The FTIR spectra confirm that the existence of Fe-O stretching vibration in the range frequency of 658 cm<sup>-1</sup>-506 cm<sup>-1</sup>.

© 2018 Physics Education, UIN Raden Intan, Lampung, Indonesia.

**Keywords:** characterization, coprecipitation, microstructure, iron sand, synthesis.

## INTRODUCTION

Ferrite (MFe<sub>2</sub>O<sub>4</sub>) is one group of oxide materials that for three decades has received a lot of attention from researchers to study. This is because ferrite nanoparticles have unique physical properties, including unique mechanical, optical, electrical, acoustic, and magnetic properties compared to other material groups. Ferrite chemical properties such as the stability of chemical reactions and photocatalysis are also unique (Jaswal, Singh, & Jaswal, 2014).

Ferrite materials are in various forms, such as nanoparticles, nanoribbons,

nanosheets, and nanowires. Nanoparticles are a form of ferrite material in the form of particles with various morphologies, for example like solid balls.

One example of ferrite nanoparticles is magnetite (Fe<sub>3</sub>O<sub>4</sub>). The Fe<sub>3</sub>O<sub>4</sub> nanoparticles consist of divalent cation Fe<sup>2+</sup> and trivalent Fe<sup>3+</sup> cations. This nanoparticle has an inverse spinel crystal structure with the formula of cation distribution that is (Fe<sup>3+</sup>)<sub>tet</sub> [Fe<sup>2+</sup> Fe<sup>3+</sup>]<sub>octa</sub> O<sub>2</sub><sup>-4</sup> (Rani & Varma, 2015). The geometry of the crystal structure of Fe<sub>3</sub>O<sub>4</sub> nanoparticles can be illustrated in Figure 1.

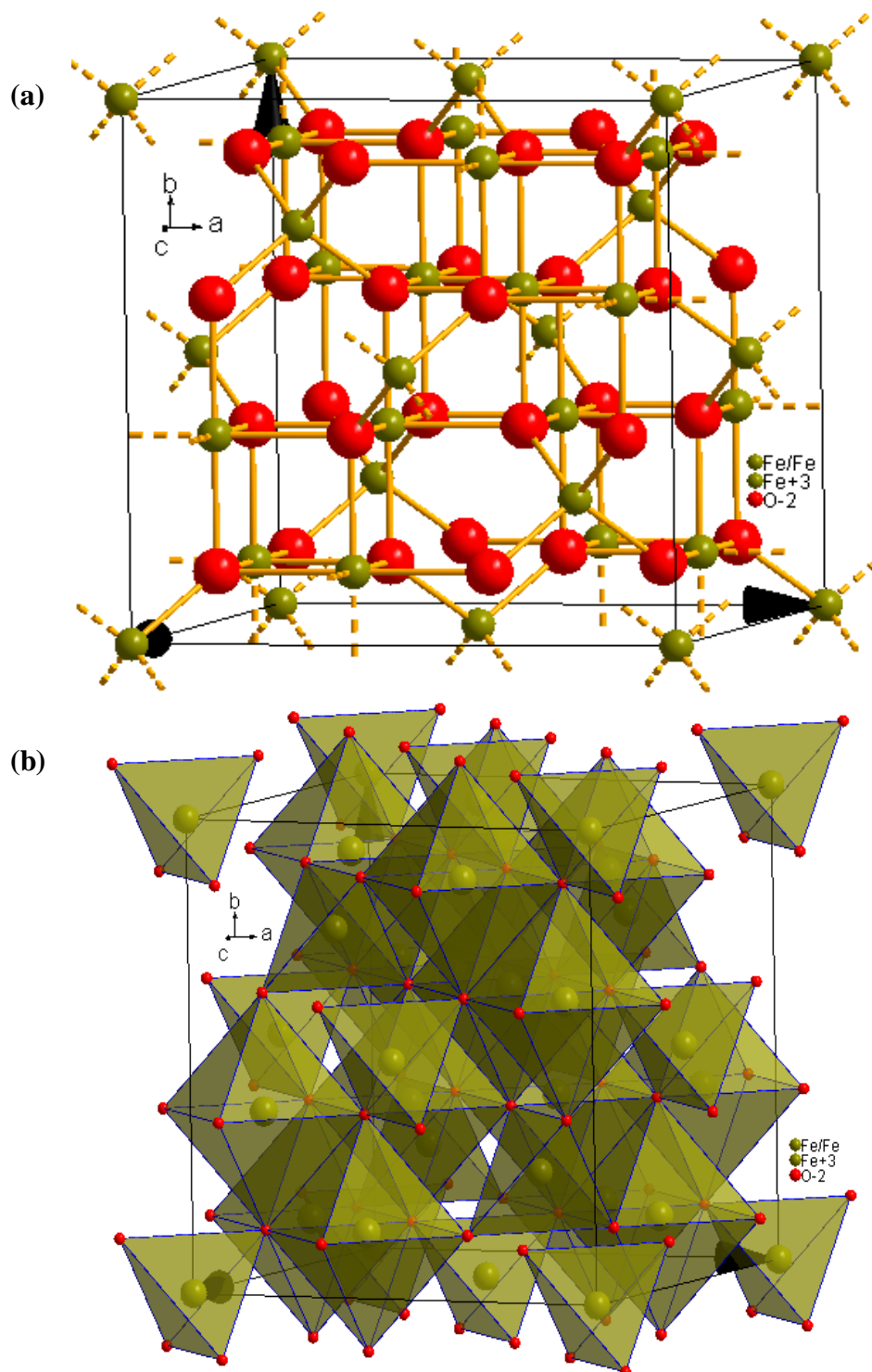


**Figure 1.** Crystal structure inverse spinel  $\text{Fe}_3\text{O}_4$ : (a) crystal structure of  $\text{Fe}_3\text{O}_4$ , (b) octahedral and tetrahedral sub lattice structures (Montoro, 1938)

Based on its physical and psycho-chemical properties, the  $\text{Fe}_3\text{O}_4$  nanoparticles have various potential applications. In the medical field, the  $\text{Fe}_3\text{O}_4$  can be used as a contrast agent for MRI images, drug delivery agents, and

cancer thermotherapy agents. In the environmental field, the  $\text{Fe}_3\text{O}_4$  can be used as catalysis to reduce organic and inorganic compounds found in contaminated liquid substances. In this field, the  $\text{Fe}_3\text{O}_4$  can also be used as a

magnetic adsorbent for dissolved heavy metal ions in a liquid (Li et al., 2010; Tang & Lo, 2013; Xu et al., 2012). In the field of electronics and instrumentation, the  $\text{Fe}_3\text{O}_4$  can be applied as the main material in the manufacture of inductor coils, electromagnetic wave coating materials, and microwave absorber (Valenzuela, 2012).

The superior physical and chemical properties of  $\text{Fe}_3\text{O}_4$  nanoparticles are influenced by various factors, such as microstructure, grain morphology structure and particle size (Jianling, Decai, Shaolan, Hongchao, & Cui, 2011). Microstructure factors include crystal structure, length of crystal lattice parameters, lattice defects, and crystal density, including the various phases of the nanoparticles. The microstructure factor is influenced by several factors, namely the type of starting material, synthesis method, precursor mole composition, synthesis temperature, and additional heat treatment such as annealing, sintering, or calcination (Mascolo, Pei, & Ring, 2013).

Various methods have been used to synthesize  $\text{Fe}_3\text{O}_4$  nanoparticles, such as coprecipitation (Frey, Peng, Cheng, & Sun, 2009; Jianling et al., 2011; Mascolo et al., 2013; Wang, Wei, & Qu, 2013) thermal decomposition and metal reduction reactions (Taufiq, Triwikantoro, Pratapa, & Darminto, 2008). The coprecipitation method is the easiest chemical method to do compared to other methods because the coprecipitation method does not involve a high synthesis temperature ( $> 150^\circ\text{C}$ ), a long synthesis time, and the process is not complicated (Nuzully, Kato, Iwata, & Suharyadi, 2013).

The use of coprecipitation method in the synthesis of  $\text{Fe}_3\text{O}_4$  nanoparticles involves precursors in the form of anhydrous metal salt compounds (metal salt), such as  $\text{FeCl}_3 \cdot 6\text{H}_2\text{O}$  as providers of  $\text{Fe}^{3+}$  and  $\text{FeCl}_2 \cdot 4\text{H}_2\text{O}$  cations as providers

of  $\text{Fe}^{2+}$ , or  $\text{Fe}_2\text{SO}_4 \cdot 6\text{H}_2\text{O}$  cations as  $\text{Fe}^{2+}$  providers (Dewi, Puji, & Suharyadi, 2014; Triwikantoro, Yahya, & Darminto, 2011). The synthetic anhydrous compounds can be replaced with natural materials such as iron sand containing  $\text{Fe}^{2+}$  and  $\text{Fe}^{3+}$  metals. Several studies have succeeded in synthesizing  $\text{Fe}_3\text{O}_4$  nanoparticles using natural materials of iron sand, such as (A. Taufik et al., 2017; Bilalodin, Sunardy, & Effendy, 2013; Setiadi et al., 2016; Taufiq et al., 2008; Triwikantoro et al., 2011).

In this research,  $\text{Fe}_3\text{O}_4$  nanoparticles will be synthesized from natural materials of iron sand found in Wari Ino Beach, Tobelo Subdistrict, North Halmahera as precursors in providing  $\text{Fe}^{2+}$  and  $\text{Fe}^{3+}$  ions. The availability of iron sand in Wari Ino Beach is very abundant, and until now there has been no research that covers the metal mineral content of iron  $\text{Fe}^{2+}$  and  $\text{Fe}^{3+}$ , especially using them as a base for the synthesis of  $\text{Fe}_3\text{O}_4$  nanoparticles. Information about the mineral content of iron sand from Wari Ino Beach is very interesting to study, and the process of synthesizing  $\text{Fe}_3\text{O}_4$  nanoparticles using those sand needs to be done in the framework of its application for various fields, especially the environment. Microstructure studies of  $\text{Fe}_3\text{O}_4$  nanoparticles from iron sand are important to be carried out in order to provide empirical justification of their physical and chemical properties.

This study focuses on the synthesis and microstructure studies of  $\text{Fe}_3\text{O}_4$  nanoparticles including crystal structure, lattice parameters (lattice parameters), crystal spacing, X-ray density, lattice strain, and texture coefficient.

## METHOD

### Apparatus and Materials

The apparatus used to synthesize  $\text{Fe}_3\text{O}_4$  nanoparticles are 250 ml beaker, 100 ml beaker, spatula rod, drop pipette, pour bottle, petri dish, magnetic hot plate,

oven, thermometer, pH meter, and digital scales. The characterization tools used for the identification of elemental composition, the crystal structure and functional group bonds of nanoparticle are X-Ray Fluorescence (XRF), X-Ray Diffractometer (XRD) and Fourier Transform Infrared (FTIR) Spectrophotometer, consecutively. The material used for the synthesis of  $\text{Fe}_3\text{O}_4$  nanoparticles is iron sand from Wari Ino Beach.

### Sample Preparation Procedure

The synthesis process of  $\text{Fe}_3\text{O}_4$  nanoparticles can be illustrated such as Figure 2. The process was started by dissolving iron sand (total mass of 10 grams) into 20 ml HCl (6M) and stirred while heating at  $70^\circ\text{C}$  for 30 minutes on a hot plate stirrer with the aim of forming a solution of  $\text{FeCl}_3$  and  $\text{FeCl}_2$ . A total of 3.0 grams of NaOH were dissolved in 20 ml

of distilled water. The NaOH solution was heated for 10 minutes after being sterilized for 15 minutes. The iron sand solution is dropped into a NaOH solution using a dropping pipette while being sterilized and heated with a synthesis temperature of  $56^\circ\text{C}$ .

After an hour, black deposits will form. The temperature of this precipitate is naturally derived until it reaches thermal equilibrium with room temperature. The precipitate was rinsed with distilled water and deposited again on a permanent magnet for 30 minutes. The rinsing process is carried out five times. The precipitate is then in the oven at a temperature of  $100^\circ\text{C}$  for 3 hours. This slurry heating process will produce solid pieces which are a collection of  $\text{Fe}_3\text{O}_4$  nanoparticles. The chips are crushed to produce nanoparticle powder which is further characterized.

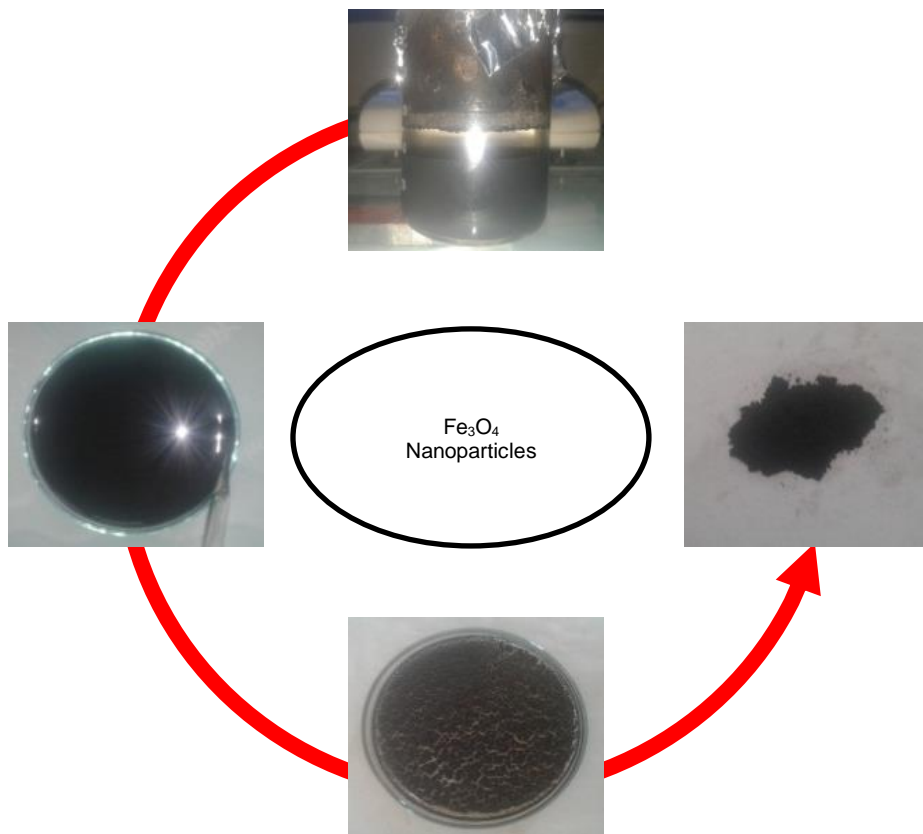


**Figure 2.** The process of synthesis of  $\text{Fe}_3\text{O}_4$  sample

**Characterization of Nanoparticles**

The elemental composition of the samples was identified using the XRF instrument. Characterization of a microstructure of nanoparticles including crystal structure, lattice parameters, crystal spacing distance, X-ray density, lattice strain, and texture coefficient was carried out using XRD. Nanoparticle functional groups were characterized using FTIR.

**RESULT AND DISCUSSION**

**Qualitative Description of Fe<sub>3</sub>O<sub>4</sub> Nanoparticles**

The sample obtained from the synthesis of Fe<sub>3</sub>O<sub>4</sub> nanoparticles in the form of fine black powder. The black color is one of the characteristics of Fe<sub>3</sub>O<sub>4</sub> nanoparticles. In addition, other characteristics have also been observed, namely the response of powder nanoparticles when tested with an external magnet. Powder nanoparticles

experience a magnetic attraction to external magnets.

**The Elemental Composition of Fe<sub>3</sub>O<sub>4</sub>**

The XRF characterization results of Fe<sub>3</sub>O<sub>4</sub> nanoparticle samples provide information regarding the type and composition of the elements contained in the sample. The types of these elements are determined based on characteristic X-ray energy radiated by the atoms contained in the material. Meanwhile, the element composition is indicated by the peak height of the spectra as shown in Figure 3.

The XRF spectra confirmed the presence of fourteen types of elements contained in Fe<sub>3</sub>O<sub>4</sub> nanoparticle samples, namely aluminum (Al), phosphorus (P), calcium (Ca), titanium (Ti), vanadium (V), chromium (Cr), manganese (Mn), Iron (Fe), Nickel (Ni), copper (Cu), Zinc (Zn), Rubidium (Rb), rhenium (Re) and bismuth (Bi) are presented in Table 1.

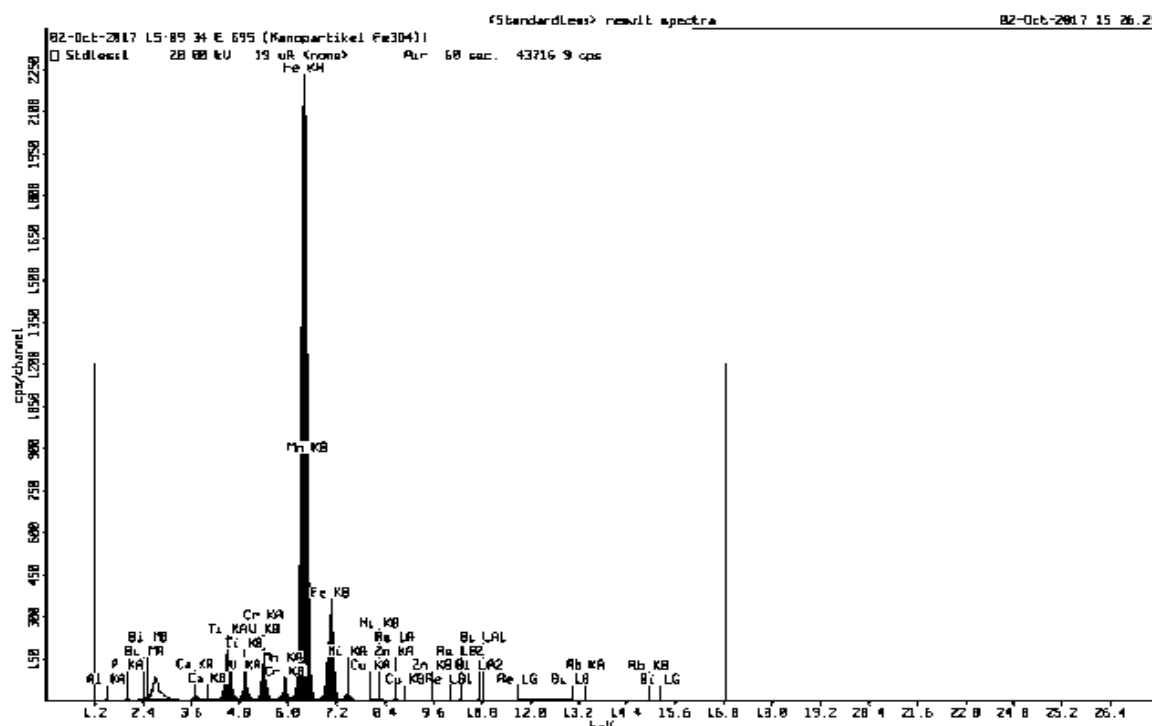


Figure 3. The XRF Spectra of Fe<sub>3</sub>O<sub>4</sub> nanoparticles

According to the results, the most elemental content is iron (Fe) with an elemental composition of 87.35%, while the least elemental content is zinc (Zn) with an elemental composition of 0.08%. The composition of Fe metal in the sample results of this study is greater than the results obtained by (Bilalodin et al., 2013; Linda & Pratapa, 2014; Triwikantoro et al., 2011). (Triwikantoro et al., 2011) used the coprecipitation synthesis method at 80°C for an hour and produced Fe<sub>3</sub>O<sub>4</sub> samples with Fe content of 76.92%. Bilalodin et al. (2013) obtained a Fe content of 21.00%. Meanwhile, Kartika and Pratama (2014) using the dissolved metal method of hydrochloric acid produced Fe<sub>3</sub>O<sub>4</sub> samples with Fe composition of 87.00%. The difference in results can be caused by differences in synthesis methods and synthesis parameters used in producing Fe<sub>3</sub>O<sub>4</sub> nanoparticles. Therefore, the selection of the right synthesis method and the value of the synthesis parameter is very influential mainly on the composition and physical properties of Fe<sub>3</sub>O<sub>4</sub> produced.

**Table 1.** Elemental composition of sample

No	Element	Composition (%)
1	Al	1.00
2	P	0.26
3	Ca	0.61
4	Ti	4.73
5	V	0.63
6	Cr	1.75
7	Mn	0.56
8	Fe	87.35
9	Ni	1.34
10	Cu	0.14
11	Zn	0.08
12	Rb	0.46
13	Re	0.20
14	Bi	0.68

Based on the results in Table 1, the Fe<sub>3</sub>O<sub>4</sub> nanoparticles still contained impurities such as Al, P, Ca, Ti, V, Cr, Mn, Ni, Cu, Zn, Rb, Re, and Bi. This

states that the process of separating magnetic iron material with nonmagnetic elements has not yet occurred optimally. The existence of these elements does not significantly affect the physical and psycho-chemical properties of Fe<sub>3</sub>O<sub>4</sub> nanoparticles.

### The Microstructural properties of Fe<sub>3</sub>O<sub>4</sub>

X-ray diffraction test was carried out to identify the microstructure and crystal structure of Fe<sub>3</sub>O<sub>4</sub> nanoparticles which included crystallite size, lattice parameters, crystal density, lattice strain, and texture coefficient. X-ray diffraction data of Fe<sub>3</sub>O<sub>4</sub> samples were adjusted to the standard data of Joint Committee Powder Diffraction Standard (JCPDS) no. 11-0614.

The X-ray diffraction test results of Fe<sub>3</sub>O<sub>4</sub> nanoparticles give data in the form of 2θ diffraction angle and intensity. The diffraction pattern was plotted by using Origin 9.0 for Windows software as shown in Figure 4. The diffraction pattern shows the existence of seven diffraction peaks. The seven diffraction peaks state the electron diffraction process that occurs in the diffraction (hkl) plane of Fe<sub>3</sub>O<sub>4</sub> nanoparticles, namely fields (220), (311), (400), (422), (511), (440), and (533) which are characteristics of Fe<sub>3</sub>O<sub>4</sub> nanoparticle diffraction pattern according to JCPDS standard data 11-0614. In this diffraction pattern, no diffraction peaks were found in phases other than Fe<sub>3</sub>O<sub>4</sub>, so it can be concluded that the pure synthesized samples consisted of Fe<sub>3</sub>O<sub>4</sub> nanoparticles.

The calculation results of the crystal lattice of Fe<sub>3</sub>O<sub>4</sub> nanoparticle approach the standard value according to JCPDS number 11-0614, which is 8.34 ± 0.049 Å. This value is equivalent to the results of research by Darminto et al (2011), Setiadi et al (2016) and the standard value of the JCPDS data is 8.396 Å. The volume of the Fe<sub>3</sub>O<sub>4</sub> crystal lattice is

$0.589 \times 10^{-27} \text{ m}^3$ . The average size of  $\text{Fe}_3\text{O}_4$  nanoparticles is  $24.25 \pm 0.042 \text{ nm}$ . The crystal lattice density ( $\rho_x$ )  $\text{Fe}_3\text{O}_4$  is

$5.232 \times 10^3 \text{ kg/m}^3$  and the strain value that occurs in the lattice ( $\epsilon$ ) is  $1.413 \times 10^{-3} / \text{line}$ .

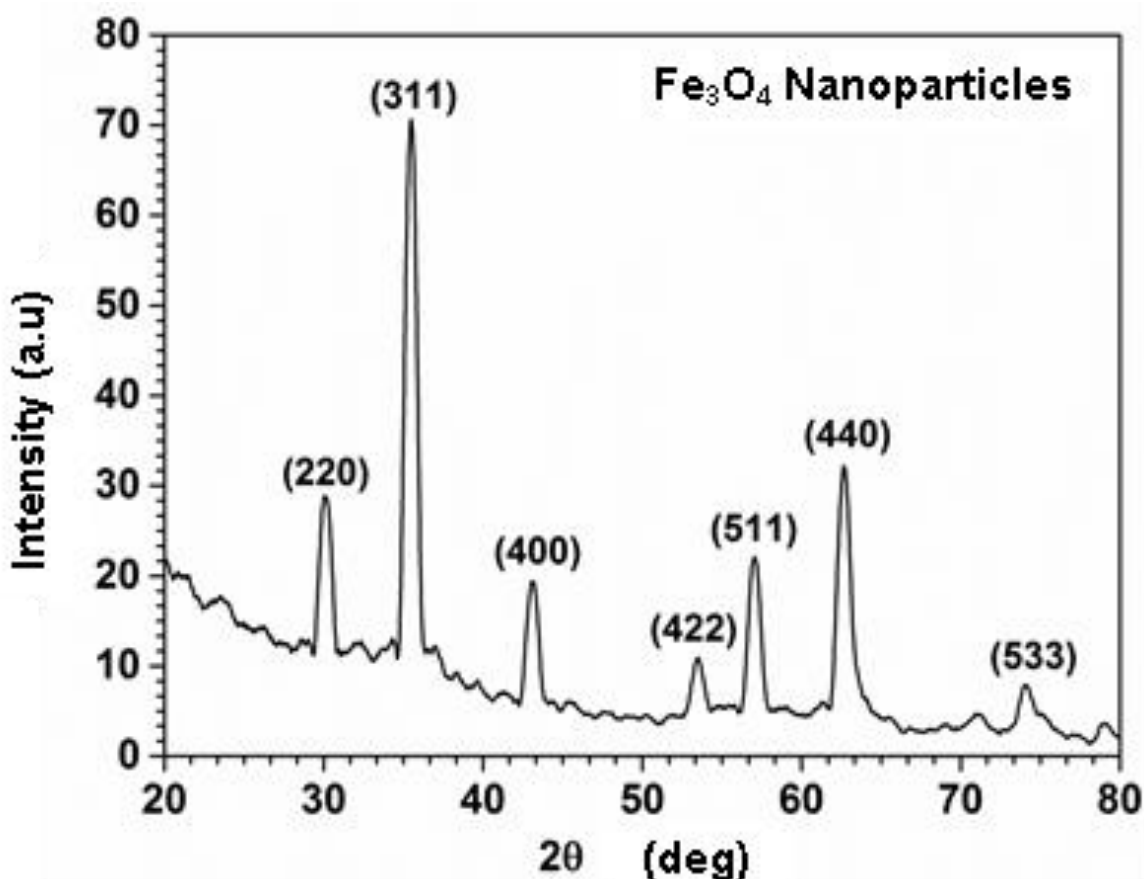


Figure 4. The XRD pattern of  $\text{Fe}_3\text{O}_4$  nanoparticles

The degree of crystallinity of  $\text{Fe}_3\text{O}_4$  samples can be identified based on data of texture coefficient (TC) of relating diffraction peak (hkl). Figure 5 shows the TC value (hkl) for each orientation direction of  $\text{Fe}_3\text{O}_4$  nanoparticles crystal grains. The results of calculation of TC values (hkl) diffraction peaks in fields (220), (311), (400), (422), (511), (440) and (533) respectively (0.9), (2, 3), (0.7),

(0.4), (0.8), (1.2) and (0.6). From the calculation of the TC (hkl) value there are five diffraction peaks which have a TC value (hkl) smaller than 1 of them namely the diffraction peaks of the fields (220), (440), (422), (511) and (533) indicates that the growth of  $\text{Fe}_3\text{O}_4$  nanoparticles at the diffraction peak tends to be very low and the direction of the crystal grain orientation is not regular.

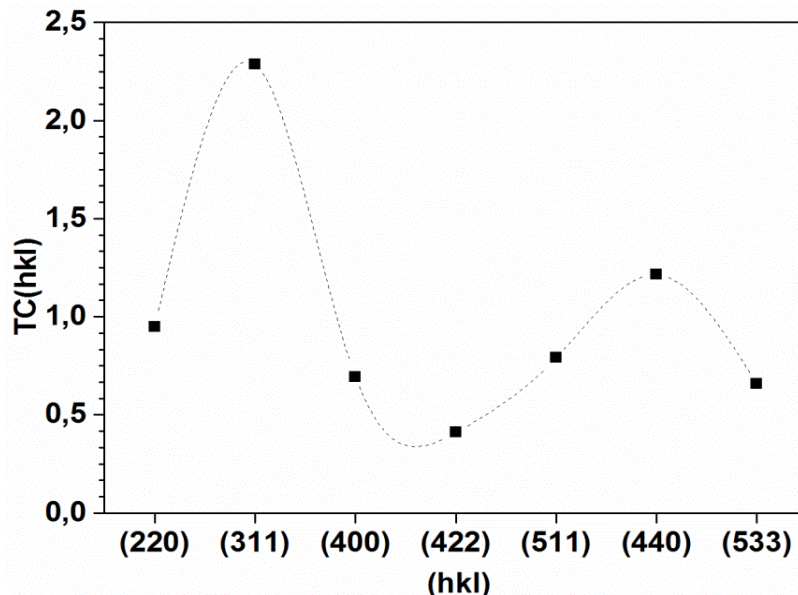


Figure 5. Texture coefficient of the XRD peaks of the Fe<sub>3</sub>O<sub>4</sub> nanoparticle

4. Functional Groups Bonds of Fe<sub>3</sub>O<sub>4</sub>

The Fourier Transform Infrared Spectroscopy (FTIR) test results provide information about the infrared spectra absorption profile on Fe<sub>3</sub>O<sub>4</sub> nanoparticle samples. Characterization of Fe<sub>3</sub>O<sub>4</sub> nanoparticles FTIR was carried out for the 500 cm<sup>-1</sup>- 4000 cm<sup>-1</sup> wavenumber interval. The data plot transmits the wave number of infrared light in the form of sharp absorption peaks in certain wavenumbers resulting from the vibration of certain functional groups, as shown in Figure 6 and Table 2.

The stretching vibration of Fe-O functional groups occurs for absorption of infrared wavenumbers in the range 506 cm<sup>-1</sup>- 658 cm<sup>-1</sup>. These results are consistent with the findings of (Setiadi et al., 2016). In the wave number interval 1672 cm<sup>-1</sup> - 1367 cm<sup>-1</sup> it is identified the occurrence of bending vibration of the H-O-H group, while the O-H group vibrates stretching at a wave number interval of 3028 cm<sup>-1</sup>- 3400 cm<sup>-1</sup>. At wave number interval 2920 cm<sup>-1</sup> - 2855 cm<sup>-1</sup>, stretching vibration of C-H group is identified.

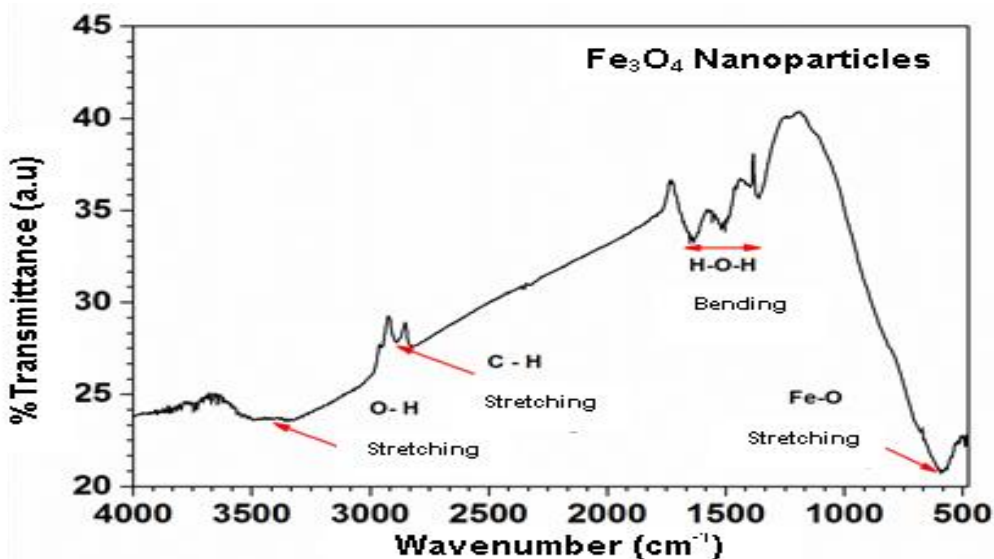


Figure 6. The FTIR Spectra of Fe<sub>3</sub>O<sub>4</sub> nanoparticle



**Table 2.** Functional group bonds of Fe<sub>3</sub>O<sub>4</sub> nanoparticles

No	Wavenumber (cm <sup>-1</sup> )	Functional group
1	658 – 506	Fe – O stretching
2	1672 – 1367	H – O – H bending
3	3028 – 3400	O – H stretching
4	2920 – 2855	C – H stretching

## CONCLUSION

The Fe<sub>3</sub>O<sub>4</sub> nanoparticles have been successfully synthesized using the coprecipitation method at 56°C. The Fe<sub>3</sub>O<sub>4</sub> samples synthesized from the iron sand of Wari Ino Beach contain elements of Fe at 87.35%. The Fe<sub>3</sub>O<sub>4</sub> nanoparticles have a spinel cubic crystal structure. The average crystallite size (*t*) of Fe<sub>3</sub>O<sub>4</sub> nanoparticles was 24.25 ± 0.42 nm, and the crystal lattice (*a<sub>ex</sub>*) parameter value was 8.34 ± 0.049 Å. The appearance of stretching vibration of the Fe-O functional group at a wave number of 658 cm<sup>-1</sup> - 506 cm<sup>-1</sup> also shows the success of the formation of Fe<sub>3</sub>O<sub>4</sub> nanoparticles.

## ACKNOWLEDGMENT

The author would like to thank the staff of Laboratorium IPA Terpadu Universitas Halmahera for providing opportunities using the research facilities, staff of the Mineral Laboratory and Advanced Materials of the Mathematics and Natural Sciences Faculty of Malang State University which helped provide facilities for characterizing Fe<sub>3</sub>O<sub>4</sub> nanoparticles, as well as the Magnetic Nanomaterial Research Group UGM for providing the materials.

## REFERENCES

Taufik, A., Saputro, R.E., Sunaryono, S., Hidayat, N., Hidayat, A., Mufti, N., Diantoro, M., Patriati, A., Mujamilah, M., Putra, E. G. R., & Nur, H. (2017). Fabrication of Magnetite Nanoparticles Dispersed

in Olive Oil and Their Structural and Magnetic Investigations. In IOP Conf. Series: Materials Science and Engineering. Malang: IOP Publishing Ltd. <https://doi.org/10.1088/1757-899X/202/1/012008>.

Bilalodin, Sunardy, & Effendy, M. (2013). Analisis Kandungan Senyawa Kimia dan Uji Sifat Magnetik Pasir Besi Pantai Ambal. *Jurnal Fisika Indonesia*, 17, 29–31.

Dewi, S., Puji, F., & Suharyadi, E. (2014). Studi Penurunan Kadar Logam Fe dan Co pada Limbah Cair dengan Sistem Purifikasi Berbasis Adsorben Nanopartikel Magnetik Fe<sub>3</sub>O<sub>4</sub>. *Jurnal Fisika Indonesia*, 18, 16–19.

Frey, N. A., Peng, S., Cheng, K., & Sun, S. (2009). Magnetic Nanoparticles: Synthesis, Functionalization, and Applications in Bioimaging and Magnetic Energy Storage. *Chemical Society Review*, 2532–2542. <https://doi.org/10.1039/b815548h>.

Jaswal, L., Singh, B., & Jaswal, L. (2014). Ferrite materials: A Chronological Review. *Journal of Integrated Science & Technology*, 2(2), 69–71.

Jianling, L. I., Decai, L. I., Shaolan, Z., Hongchao, C. U. I., & Cui, W. (2011). Analysis of the Factors Affecting the Magnetic Characteristics of Nano-Fe<sub>3</sub>O<sub>4</sub> Particles. *Chinese Science Bulletin*, 56(8), 803–810. <https://doi.org/10.1007/s11434-010-4126-z>.

Li, J., Fan, M., Brown, R. C., Van, J. H., Wang, J., Wang, W., & Song, Y. (2010). Synthesis, Properties, and Environmental Applications of Nanoscale Iron-Based Materials: A Review. *Critical Reviews in Environmental Science and Technology*, 36, 37–41.

Linda, D., & Pratapa, S. (2014). Sintesis

- Fe<sub>2</sub>O<sub>3</sub> dari Pasir Besi dengan Metode Logam Terlarut Asam Klorida. *Jurnal Sains Dan Seni Pomits*, 3(2), 33–35.
- Mascolo, M. C., Pei, Y., & Ring, T. A. (2013). Nanoparticles in a Large pH Window with Different Bases. *Materials*, 6, 5549–5567. <https://doi.org/10.3390/ma6125549>.
- Montoro. (1938). Miscibilita Fra Gli Ossidi Salini di Ferroe di Manganese. *Gazzetta Chimica Italiana*, 68, 728–733.
- Nuzully, S., Kato, T., Iwata, S., & Suharyadi, E. (2013). Pengaruh Konsentrasi Polyethylene Glycol (PEG) pada Sifat Kemagnetan Nanopartikel Magnetik PEG-Coated Fe<sub>3</sub>O<sub>4</sub>. *Jurnal Fisika Indonesia*, 17, 35–40.
- Rani, S., & Varma, G. D. (2015). Superparamagnetism and Metamagnetic transition in Fe<sub>3</sub>O<sub>4</sub> Nanoparticles Synthesized via Coprecipitation Method at Different pH. *Physica B: Physics of Condensed Matter*. <https://doi.org/10.1016/j.physb.2015.05.016>.
- Setiadi, E. A., Sebayang, P., Ginting, M., Sari, A. Y., Kurniawan, C., Saragih, S. ., & Simamora, P. (2016). The synthesization of Fe<sub>3</sub>O<sub>4</sub> Magnetic Nanoparticles Based on Natural Iron Sand by Coprecipitation Method for the Used of the Adsorption of Cu and Pb Ions. *Journal of Physics: Conference Series*. <https://doi.org/10.1088/1742-6596/776/1/012020>.
- Tang, S. C. N., & Lo, I. M. C. (2013). Magnetic nanoparticles : Essential Factors for Sustainable Environmental Applications. *Water Research*, 47(8), 2613–2632. <https://doi.org/10.1016/j.watres.2013.02.039>.
- Taufiq, A., Triwikantoro, T., Pratapa, S., & Darminto. (2008). Sintesis Partikel Nano Fe<sub>3-x</sub>Mn<sub>x</sub>O<sub>4</sub> Berbasis Pasir Besi dan Karakterisasi Struktur serta Kemagnetannya Sintesis Partikel Nano Fe<sub>3-x</sub>Mn<sub>x</sub>O<sub>4</sub> Berbasis Pasir Besi. *Jurnal Nanosains & Nanoteknologi*, 1(2).
- Triwikantoro, Yahya, & Darminto. (2011). Synthesis of Fe<sub>3</sub>O<sub>4</sub> Nanoparticles from Iron Sands and Effects of Ni and Zn Substitution on Structures and Magnetic Properties. *Journal of Materials Science and Engineering A*, 1(2), 182–189.
- Valenzuela. (2012). Novel Applications of Ferrites. *Physics Research International*, 2012, 9. <https://doi.org/10.1155/2012/591839>.
- Wang, B., Wei, Q., & Qu, S. (2013). Synthesis and Characterization of Uniform and Crystalline Magnetite Nanoparticles via Oxidation-precipitation and Modified coprecipitation Methods. *International Journal of Electrochemical Science*, 8, 3786–3793.
- Xu, P., Ming, G., Lian, D., Ling, C., Hu, S., & Hua, M. (2012). The Use of Iron Oxide Nanomaterials in Wastewater Treatment: A Review. *Science of the Total Environment*, 424, 1–10. <https://doi.org/10.1016/j.scitotenv.2012.02.023>.